Capacitor-less D-STATCOM for Voltage Profile Improvement in a SmartGrid Distribution Network with High PV Penetration

Wesam Rohouma
Electrical Engineering Department
College of EngineeringTechnology & Industrial Trades
University of Doha for Science & Technology
Doha, Qatar
wesam.rohouma@ieee.org

Robert S. Balog
Renewable Energy & Advanced Power Electronics Research Laboratory
Texas A&M University at Qatar
Doha, Qatar
robert.balog@ieee.org

Miroslav M. Begovic
Department of Electrical & Computer Engineering
Texas A&M University at Qatar
College Station, Texas USA
begovic@tamu.edu

Aaqib Ahmad Peerzada
Department of Electrical & Computer Engineering
Texas A&M University at Qatar
College Station, Texas USA
peerzada@tamu.edu

***Abstract* — Distributed photovoltaic (PV) systems are can provide a multitude of advantages to both utilities and consumers facilitated through the smart grid framework. However, due to the very nature of its variability and weather dependencies, the large-scale integration of this type of distributed generation has created challenges for the network operator in terms of reverse power flow and voltage rise in distribution feeders. One of the technologies to overcome these issues is to use reactive power compensators to keep the voltage profile within the limits set by the standards. Distribution static synchronous compensator (D-STATCOM) based matrix converter (MC) is proposed for use in low voltage distribution network to provide the required voltage support. This technology is reliable and has a long service life as it employs inductive energy storage instead of the capacitive elements which will improve the system reliability, controlled by finite-set model predictive control. Experimental results are provided to show the effectiveness of the proposed technology.**

Keywords— D-STATCOM, Voltage profile, Reactive power compensation, Model predictive control, Matrix converter.

I. Introduction

Voltage regulation is a critical factor in improving the reliability and security of any electrical power system. In conventional power system configuration, the power flows from generation through transmission and distribution network to the end-user. Custumers connected at the end of the low voltage distribution network will experience poor voltage regulation due to voltage drop in distribution cables. With the increased penetration of the non-dispatchable distributed PV energy resources in the low voltage network more active power will be fed back to the grid, and this reverse power flow in the feeder will cause number of power quality issues, and one of these issues is the voltage rise in the feeder [1, 2].

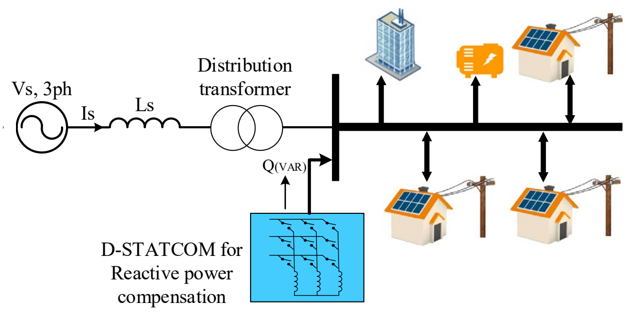

Fig. 1 One-line diagram of distribution system. The proposed D-STATCOM is shunt connected at a specific bus to provide the required compensation.

Traditionally, various control devices have been used to regulate the voltage in the distribution network including on-load tap changer (OLTC), capacitor banks, and D-STATCOMs [3-5]. A D-STATCOM is a fast response power electronics device that can provide flexible voltage regulation, power factor correction, and harmonics mitigation in the distribution network. However, the available D-STATCOM in the market is based on voltage source converter (VSC) with electrolytic capacitors. These capacitors are subjected to accelerated failures especially in hot/arid environments [6-8]. According to [9-11], 30% of the failures that occur in power electronics are due to DC electrolytic capacitors.

In this paper, a capacitor-less D-STATCOM based matrix converter as shown in Fig.1 will be used to provide the required reactive power compensation in low voltage network to improve the voltage profile in the distribution feeder. Experimental results will be presented using 7.5KVA experimental prototype.

II. Proposed D-STATCOM System

The proposed D-STATCOM is shown in Fig.1. It consists of a three-phase supply with series impedance L_s connected to the three-phase load with large renewable penetration and inductive loads. The proposed D-STATCOM system consists of a three-phase matrix converter system connected to the point of common coupling (PCC) through an input filter and the MC output is connected to an inductive energy storage element L_{MC}. The proposed D-STATCOM is controlled using finite control set model predictive control (FCS-MPC) programmed in the dSPACE control platform.

A. Matrix converter model

Matrix converter is a type of power electronics converters that can perform direct AC/AC power conversion without the use of electrolytic DC capacitors, and this will increase its reliability and service life in comparison to the traditional VSC [12]. As shown in Fig. 2, the power circuit of the matrix converter consists of nine bidirectional switches each comprised of two IGBT and diode pairs connected in antiparallel to support bidirectional current flow. The MC is connected to the distribution network through an input filter to prevent the high-frequency switching harmonics from propagating to the network. The output voltages and input currents of the MC were calculated according to (1), (2) and (3) as a function of MC input voltages, output currents and the switching function. The inductive load constrains the switching to avoid interruption of MC output current. The voltage-source input constrains the switching to avoid shorting the input phases. This constraint is expressed as:

$$S_{Ay}+S_{By}+S_{Cy}=1 \quad \text{where} \quad y \in (a,b,c) \tag{1}$$

$$\begin{bmatrix} v_{oa} \\ v_{ob} \\ v_{oc} \end{bmatrix} = \begin{bmatrix} S_{Aa} & S_{Ba} & S_{Ca} \\ S_{Ab} & S_{Bb} & S_{Cb} \\ S_{Ac} & S_{Bc} & S_{Cc} \end{bmatrix} \cdot \begin{bmatrix} V_{SA} \\ V_{SB} \\ V_{SC} \end{bmatrix} \tag{2}$$

$$\begin{bmatrix} I_{inA} \\ I_{inB} \\ I_{inC} \end{bmatrix} = \begin{bmatrix} S_{Aa} & S_{Ab} & S_{Ac} \\ S_{Ba} & S_{Bb} & S_{Bc} \\ S_{Ca} & S_{Cb} & S_{Cc} \end{bmatrix} \cdot \begin{bmatrix} I_{oa} \\ I_{ob} \\ I_{oc} \end{bmatrix} \tag{3}$$

where $V_{oa}(t)$, $V_{ob}(t)$ and $V_{oc}(t)$, $I_{oa}(t)$, $I_{ob}(t)$ and $I_{oc}(t)$ are the output voltages and currents of the matrix converter respectively. While, $V_{sA}(t)$, $V_{sB}(t)$ and $V_{sC}(t)$, $i_{inA}(t)$, $I_{inB}(t)$ and $I_{inC}(t)$ are the input voltages and currents of the matrix converter, and $S_{ij}(t)$ is the switching function for i is an element of (A,B,C) and j is an element of (a, b, c). Proper choice of $\boldsymbol{S}$ will lead to a phase-reversal of the current so that the inductive load appears capacitive at the input to the MC [13-15].

III. CONTROL SYSTEM

The functional-block diagram of the proposed controller is shown in Fig. 2; it consists of two stages. The first stage is the reference current detection stage and the second is the model predictive control stage. In the first stage, the voltage at the PCC is measured and the root-mean-square (rms) voltage value and angle are calculated. The instantaneous three-phase load currents are measured and decomposed into its real and reactive components using synchronous reference frame (SRF) method. or dq0 transformation method [4, 16, 17].

The voltage regulator part compares the measured PCC voltage value with the required reference and the error signal is passed to PI controller to generate the required reactive current for voltage regulation which is added to the reactive load current component as in Fig. 3. The real component of the load current consists of a DC part that represents the fundamental component of the current and the AC part that represent the harmonics. Using a high pass filter (HPF), the harmonic component can be extracted and then transformed back to the ABC reference frame to be used as a reference current for the controller.

The transformation to the d-q reference frame from the ABC reference frame is given in (4):

$$\begin{bmatrix} \mathrm{Id} \\ \mathrm{Iq} \\ \mathrm{I0} \end{bmatrix} = \sqrt{\frac{2}{3}} \begin{bmatrix} \cos(\omega t) & \cos(\omega t-2\pi/3) & (\omega t+2\pi/3) \\ -\sin(\omega t) & -\sin(\omega t-2\pi/3) & -\sin(\omega t+2\pi/3) \\ 1/\sqrt{2} & 1/\sqrt{2} & 1/\sqrt{2} \end{bmatrix} \cdot \begin{bmatrix} \mathrm{I_{LA}} \\ \mathrm{I_{LB}} \\ \mathrm{I_{LC}} \end{bmatrix} \tag{4}$$

The second stage is the MPC stage, in this stage the MPC has two functions as in Fig.1. First, it predicts the future behaviour of the system using the system model, second it minimizes the error between the reference and the predicted signals in the next sampling period. This controller is simple to implement, and it has a fast dynamic response. To predict the output currents of the MC, the model for the MC output inductors is derived:

$$L_{MC}\frac{di_o(t)}{dt} = v_o(t) - R_{LMC}i_o(t) \tag{5}$$

To approximate the derivative in (5), forward Euler method is used for each k^{th} discrete sample time steps:

$$\frac{di_o(t)}{dt} \approx \frac{i_o(k+1) - i_o(k)}{T_S} \tag{6}$$

From (5) and (6), the discrete-time model estimates the current at the next sample (k+1) is given as [18]:

$$i_o^p(k+1) = \left(1 - \frac{R_{LMC}T_s}{L_{MC}}\right)i_o(k) + \frac{T_s}{L_{MC}}v_o(k) \tag{7}$$

where R_{LMC} is the per-phase parasitic resistance of the output chokes. The input reactive power and the input current of the converter can be written in orthogonal coordinates as:

$$Q^p(k+1) = V_{s\beta}(k)i_{in\alpha}(k) - V_{s\alpha}(k)i_{in\beta}(k) \tag{8}$$

$$\begin{aligned} i_{in}^p(k+1) &= A_{q(2,1)}V_{en}(k) + A_{q(2,2)}i_{in}(k) \\ &+ B_{q(2,1)}V_s(k) + B_{q(2,2)}i_e(k) \end{aligned} \tag{9}$$

where α and β are the real and imaginary components of the associated voltage and current vectors. $i_{in}^p(k+1)$ is the

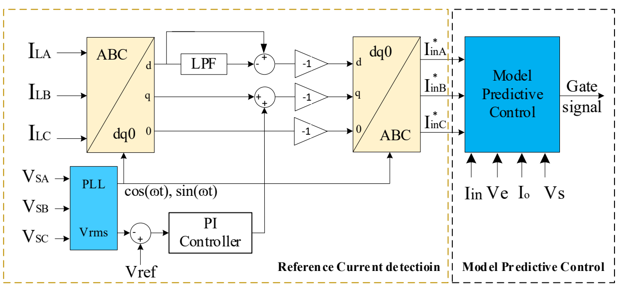

Fig. 2 Reference current detection based SRF

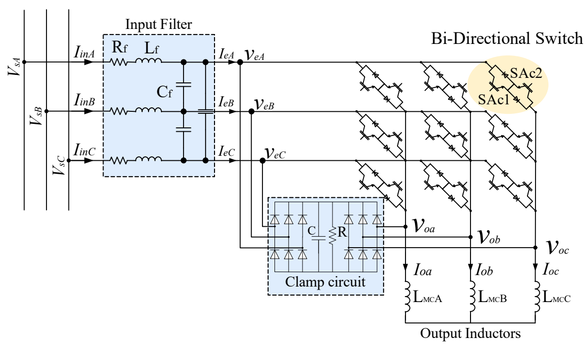

Fig. 3 Power converter power topology showing the 3x3 direct matrix converter with inductive load (L_{MC}). In this topology there is no DC-link capacitor to wear out and fail.

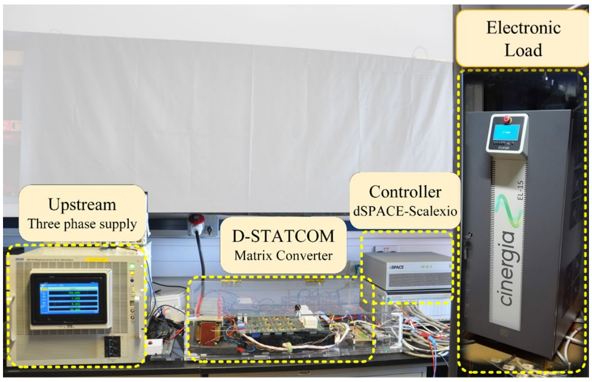

Fig. 6 Experimental setup of 7.5 kVA D-STATCOM

predicted value of the D-STATCOM input current for the sampling interval (k+1).

The cost function $\boldsymbol{J}$ is given as

$$J = \lambda_1 \left(\left| I^p_{inA} - i^*_{inA} \right| + \left| I^p_{inB} - i^*_{inB} \right| + \left| I^p_{inC} - i^*_{inC} \right| \right) + \lambda_2 \left(\left| I^p_{oa} - i^*_{oa} \right| + \left| I^p_{ob} - i^*_{ob} \right| + \left| I^p_{oc} - i^*_{oc} \right| \right) \quad (10)$$

where J is the cost function and I_{inA}, I_{inB} and I_{inC} are the MC input currents, I_{oa}, I_{ob} and I_{oc} is the MC output currents. The weight factors λ_1, λ_2 are adjusted to priorities the different parts of the cost function. Optimal tuning of these weight factor is still an open topic for research [19, 20]. In this paper, manual tuning of the weight factors is performed according to the guidelines from [20]. The current phase reversal property of the matrix converter indicates that the $i_{in}(t)$ and $i_o(t)$ are out of phase, which is the desired behaviour [14, 21-26].

IV. EXPERIMENTAL RESULTS

To verify the voltage profile regulation capability of the capacitor-less D-STATCOM, a prototype was implemented as in Fig.4 using parameters as given in Table 1. The experimental setup consists of Upstream side (12 kVA three-phase grid simulator NHR-9410), downstream side (Electronic load from Cenergia), D-STATCOM unit (7.5 kVA Matrix converter unit with three-phase inductors connected at its the output side), and control platform (dSPACE Scalexio) to control the matrix converter.

TABLE I. SYSTEM PARAMETERS

PARAMETER	VALUE
Voltage, $V_{LN,rms}$	240 V
Frequency	50Hz
Reactive Power Q (3-ph)	3000 VAR
Active power P (3-ph)	2000 to 4000 W
Power Factor p.f	0.6-1
Output chokes inductance L_{MC}	36mH
Input filter resistance Rf	2 Ω
Input filter inductance Lf	10mH
Input filter capacitor Cf/phase	12 uF
Sampling time Ts	40µs
Weight factor λ1	1
Weight factor λ2	0.2

The matrix converter unit consists of nine IGBT modules SK60GM123, isolated gate drive circuits, current direction detection circuit, clamp circuit for overvoltage protection, voltage transducers LEM LV 25-p and current transducers LEM LP 55. The dSPACE control platform consists of a processing unit and LabBox™ with 4 FPGA modules each module has 5 ADC 14bit resolution, 10 digital I/O pins and 5 analogue output pins. The MPC strategy is implemented in dSPACE Scalexio processing unit, while the measurements and four-step commutation and protection are implemented in dSPACE LabBox™ unit. dSPACE ControlDesk™ software is used to supervise and control the experiment in real-time and view and store the experimental results and modify the desired control parameters during the experiment.

It can be seen from Fig. 5 that before the D-STATCOM is connected the upstream providing the load with active power of 4000W and reactive power of 2750 VAR, while the D-STATCOM reactive power is zero. Also, the active power change in the figure is due to the injected active power of 2000W by photovoltaic system connected at the downstream side. The same experiment was repeated again with D-STATCOM is connected. It can be seen that the source reactive power is dropped from +2750 VAR to around -750 VAR and this negative reactive power are necessary to make sure that the PCC voltage is tracking its reference, and all the reactive power required by the load is provided by the shunt connected D-STATCOM. Fig.6 shows the power factor results, it can be depicted from the figure that the power factor varies from 0.6 to 0.8 as the load change when there is no and

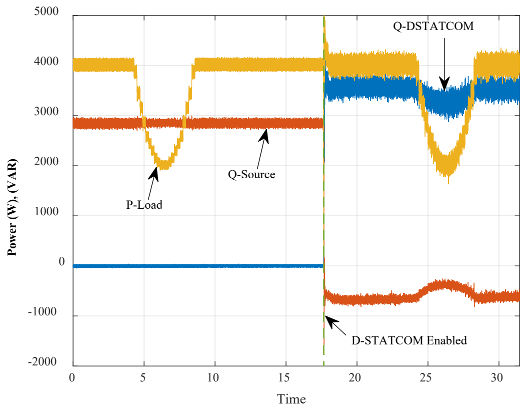

Fig. 4 Experimental results of load active power (P-Load), upstream reactive power Q-Source, and D-STATCOM reactive power Q-DSTATCM.

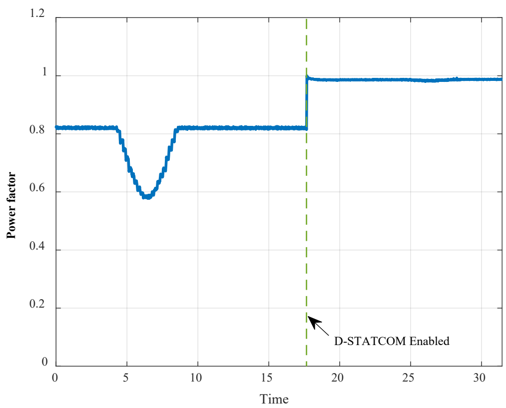

Fig. 5 Experimental results of upstream power factor, as seen by the source.

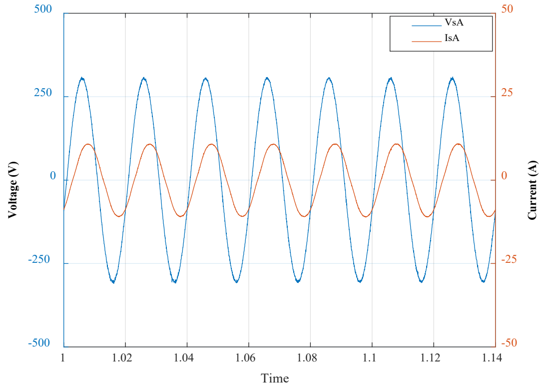

Fig. 7 Experimental results of upstream voltage (V_{SA}) and current (I_{SA}) before D-STATCOM is connected.

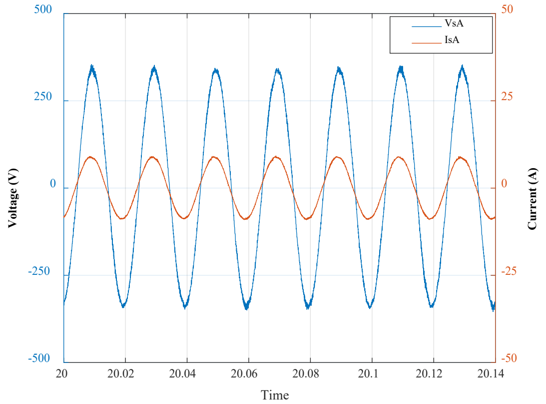

Fig. 8 Experimental results of upstream voltage (V_{SA}) and current (I_{SA}) after D-STATCOM is connected.

compensation, and after the compensator is connected the power factor becomes unity regardless of the load change.

The source voltage and current before the D-STATCOM is connected is presented in Fig.7, it could be noted that there is a phase shift between the voltage and the current. And in Fig.8 after the D-STATCOM is connected it can be seen that source current is leading the voltage due to the reverse reactive power injection to the source. Fig.9 illustrates the D-STATCOM reference and measured current, and it can be seen that controller managed to track the reference and provide the required compensation. Fig. 10 shows the PCC rms voltage, it can be noted that before the D-STATCOM is connected the PCC voltage the the recommended standard, and after the D-STATCOM is connected it starts to provide the required reactive power to keep the PCC voltage track its reference set value.

In Fig. 11 the spectrum analysis of the upstream current after the connection of D-STATCOM is shown. It can be seen, that the current THD are within the range according to the recommendation of IEEE 519 standards [27].

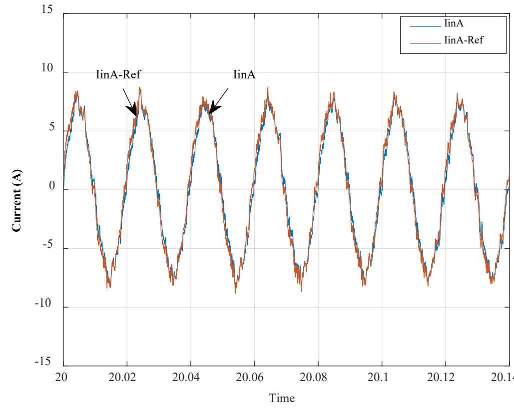

Fig. 9 Experimental results showing D-STATCOM reference input current ($I_{inA\text{-}Ref}$) and measured input current (I_{inA}).

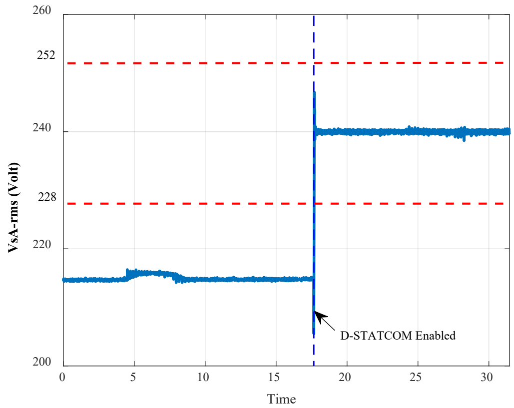

Fig. 10 Experimental results of upstream rms voltage ($V_{sA\text{-}rms}$) before and after D-STATCOM is coneected.

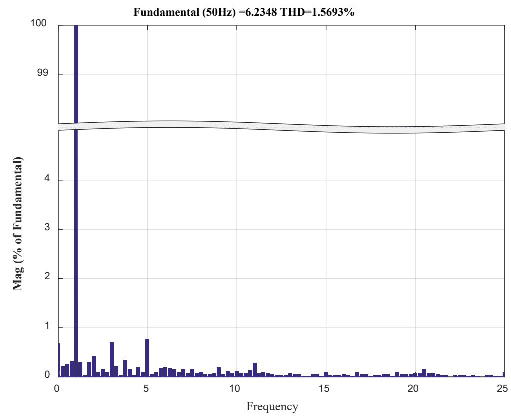

Fig. 11 Experiental results of upstream current spectra (I_{sA}) while D-STATCOM is connected.

CONCLUSION

In this paper, a capacitor-less D-STATCOM based matrix converter was used to improve the voltage profile of the low voltage distribution network with distributed PV generation. The high penetration of PV in the distribution network has a significant impact on the voltage profile. Results from the 7.5KVA experimental setup show that the proposed shunt connected capacitor-less D-STATCOM approach has the capability to improve the feeder voltage profile.

ACKNOWLEDGEMENT

This publication was made possible by NPRP grant # 13S-0213-200357 from the Qatar National Research Fund (a member of Qatar Foundation). The statements made herein are solely the responsibility of the authors.

The authors acknowledge and thank Professor Pat Wheeler and Professor Lee Empringham from the power electronics and machine control group at the University of Nottingham, UK, for their collaboration on the matrix converter prototype design and fabrication.

REFERENCES

[1] M. Thomson and D. G. Infield, "Impact of widespread photovoltaics generation on distribution systems," *IET Renewable Power Generation*, vol. 1, no. 1, pp. 33-40, Apr 2007.

[2] Y. Ueda, K. Kurokawa, T. Tanabe, K. Kitamura, and H. Sugihara, "Analysis Results of Output Power Loss Due to the Grid Voltage Rise in Grid-Connected Photovoltaic Power Generation Systems," *IEEE Transactions on Industrial Electronics*, vol. 55, no. 7, pp. 2744-2751, July 2008.

[3] M. Begovic, A. Peerzada, S. Mohan, W. Rohouma, and R. S. Balog, "Impact of Large Distributed Solar PV Generation on Distribution Voltage Control," in *Proceedings of the 52nd Hawaii International Conference on System Sciences (HICSS)*, Maui, Hawaii USA, 8-11 January 2019, pp. 3473-3482.

[4] F. Shahnia, S. Rajakaruna, and A. Ghosh, "Static Compensators (STATCOMs) in Power Systems," in *Power Systems*: Springer, 2015.

[5] C. Y. Reddy, V. Krishnakanth, R. Sanjay, V. N. V. Krishna, and R. Jayabarathi, "Laboratory implementation of Automatic Voltage Regulator," in *IEEE 2016 Biennial International Conference on Power and Energy Systems: Towards Sustainable Energy (PESTSE)*, 21-23 Jan. 2016, pp. 1-6.

[6] H. Keyhani, M. Johnson, and H. A. Toliyat, "A soft-switched highly reliable grid-tied inverter for PV applications," presented at *IEEE Applied Power Electronics Conference and Exposition (APEC)*, 16-20 March 2014.

[7] S. Harb and R. S. Balog, "Reliability of Candidate Photovoltaic Module-Integrated-Inverter (PV-MII) Topologies-A Usage Model Approach," *IEEE Transactions on Power Electronics*, vol. 28, no. 6, pp. 3019-3027, June 2013.

[8] C. Lachkar, M. Kadi, J.-P. Kouadio, M. Presle, S. El Yousfi, J.-F. Goupy, and P. Eudeline, "Failure analysis of aluminum electrolytic capacitors based on electrical and physicochemical characterizations," in *IEEE International Reliability Physics Symposium (IRPS)*, Monterey, CA, USA 02-06 April 2017, pp. 5C-1.1-5C-1.7.

[9] T. Orłowska-Kowalska, F. Blaabjerg, and J. Rodríguez, *Advanced and Intelligent Control in Power Electronics and Drives.* vol. 531: Springer, 2014.

[10] S. Yang, A. Bryant, P. Mawby, D. Xiang, L. Ran, and P. Tavner, "An industry-based survey of reliability in power electronic converters," *IEEE Transactions on Industry Applications*, vol. 47, no. 3, pp. 1441-1451, May-June 2011.

[11] L. F. Costa and M. Liserre, "Failure Analysis of the dc-dc Converter: A Comprehensive Survey of Faults and Solutions for Improving Reliability," *IEEE Power Electronics Magazine*, vol. 5, no. 4, pp. 42-51, Dec. 2018.

[12] F. Blaabjerg, "Control of Power Electronic Converters and Systems," vol. 2: Academic Press, an imprint of Elsevier Science, 2018.

[13] M. B. Shadmand, M. Mosa, R. S. Balog, and H. Abu-Rub, "Model Predictive Control of a Capacitorless Matrix Converter-Based STATCOM," *IEEE Journal of Emerging and Selected Topics in Power Electronics*, vol. 5, no. 2, pp. 796-808, June 2017.

[14] W. Rohouma, R. S. Balog, A. A. Peerzada, and M. M. Begovic, "Capacitor-less D-STATCOM for Reactive Power Compensation," in *IEEE IEEE 12th International Conference on Compatibility, Power Electronics and Power Engineering (CPE-POWERENG)*, Doha, Qatar, 10-12 April 2018.

[15] W. M. Rohouma, L. d. Lillo, S. López, P. Zanchetta, and P. W. Wheeler, "A single loop repetitive voltage controller for a four legs matrix converter ground power unit," in *IEEE Proceedings of the 14th European Conference on Power Electronics and Applications*, 30 Aug.-1 Sept. 2011.

[16] S. Bhattacharya and D. Divan, "Synchronous frame based controller implementation for a hybrid series active filter system," in *IEEE Conference Record of the Industry Applications Conference Thirtieth IAS Annual Meeting*, Orlando, FL, USA, 08-12 October 1995, pp. 2531-2540.

[17] B. Singh and V. Verma, "Selective Compensation of Power-Quality Problems Through Active Power Filter by Current Decomposition," *IEEE Transactions on Power Delivery*, vol. 23, no. 2, pp. 792-799, April 2008.

[18] J. Rodriguez and P. Cortes, *Predictive Control of Power Converters and Electrical Drives.* Wiley-IEEE Press, 2012.

[19] M. B. Shadmand, R. S. Balog, and H. A. Rub, "Auto-Tuning the Cost Function Weight Factors in a Model Predictive Controller for a Matrix Converter VAR Compensator," in *IEEE Energy Conversion Congress and Exposition (ECCE)*, Montreal, Canada, 20-24 Sept. 2015, pp. 3807 - 3814.

[20] P. Cortes, S. Kouro, B. La Rocca, R. Vargas, J. Rodriguez, J. I. Leon, S. Vazquez, and L. G. Franquelo, "Guidelines for weighting factors design in Model Predictive Control of power converters and drives," presented at *IEEE International Conference on Industrial Technology*, 10-13 February 2009

[21] W. Rohouma, R. S. Balog, A. A. Peerzada, and M. M. Begovic, "Development of a Capacitor-less D-STATCOM for Power Quality Improvement in Low Voltage Network," in *IEEE 13th International Conference on Compatibility, Power Electronics and Power Engineering (CPE-POWERENG)*, Sønderborg, Denmark, 23-25 April 2019.

[22] W. Rohouma, R. S. Balog, A. A. Peerzada, and M. M. Begovic, "Fault-Tolerant D-STATCOM based Matrix Converter," in *IEEE 2nd International Conference on Smart Grid and Renewable Energy (SGRE)*, Doha, QATAR, 19-21 November 2019, pp. 1-6.

[23] W. Rohouma, R. S. Balog, A. A. Peerzada, and M. M. Begovic, "Parallel Operation of Capacitor-less D-STATCOM to Allow More Penetration of Photovoltaic Systems in Distribution Network," in *IEEE 47th IEEE Photovoltaic Specialists Conference (PVSC)*, 15 June - 21 August 2020, pp. 2777-2782.

[24] W. Rohouma, R. S. Balog, and H. Zubi, "Application of a Capacitor-Less D-STATCOM for Power Quality Enhancement in a Typical Telecom Data Center," presented at *IEEE 3rd International Conference on Smart Grid and Renewable Energy (SGRE'22)*, 20-22 March 2022.

[25] W. Rohouma, M. Metry, R. S. Balog, A. A. Peerzada, M. Begovic, and Z. Dao, "Adaptive Model Predictive Controller to Reduce Switching Losses for a Capacitor-Less D-STATCOM," *IEEE Open Journal of Power Electronics (OJ-PEL)*, vol. 1, pp. 300-311, 2020.

[26] W. Rohouma, M. Metry, R. S. Balog, A. A. Peerzada, M. Begovic, and Z. Dao, "Analysis of the Capacitor-Less D-STATCOM for Voltage Profile Improvement in Distribution Network With High PV Penetration," *IEEE Open Journal of Power Electronics (OJ-PEL)*, vol. 3, pp. 255-270, 2022.

[27] "Std 519-2014: IEEE Recommended Practice and Requirements for Harmonic Control in Electric Power Systems," IEEE, 2014.